

Photorealistic integral photography using a ray-traced model of capturing optics

Spyros S. Athineos

Nicholas P. Sgouros

University of Athens

Department of Informatics and Telecommunications

Athens 15784, Greece

Panagiotis G. Papageorgas

Technological Educational Institute of Piraeus

Electronics Department

Athens 12244, Greece

Dimitris E. Maroulis

Manolis S. Sangriotis

Nikiforos G. Theofanous

University of Athens

Department of Informatics and Telecommunications

Athens 15784, Greece

Abstract. We present a new approach for computer-generated integral photography (IP) based on ray tracing, for the reconstruction of high quality photorealistic 3-D images of increased complexity. With the proposed methodology, all the optical elements of a single-stage IP capturing setup are physically modeled for the production of real and virtual orthoscopic IP images with depth control. This approach is straightforward for translating a computer-generated 3-D scene to an IP image, and constitutes a robust methodology for developing modules that can be easily integrated in existing ray tracers. An extension of this technique enables the generation of photorealistic 3-D videos [integral videography (IV)] and provides an invaluable tool for the development of 3-D video processing algorithms. © 2006 SPIE and IS&T. [DOI: 10.1117/1.2360692]

1 Introduction

Integral photography (IP) or integral imaging, devised by Lippmann¹ in 1908, is one of the most promising methods for displaying 3-D images, since it provides autostereoscopic viewing without eye fatigue, along with full color and continuous parallax both horizontally and vertically. The utilization of IP in 3-D imaging has been lagged for many years due to the high resolution required for reproduction and capturing devices. However, today there is a revitalizing interest in IP with the evolution in micro-optics, high resolution liquid crystal displays (LCDs), and charge-coupled devices (CCDs), together with the increased computational power of modern CPUs.

Currently, it is common practice to use computers for the generation of 3-D scenes. Computer-generated integral photography² belongs to this general category and aims to the production of integral photography images for 3-D viewing. A number of software ray tracing models have been reported^{3,4} for the generation of integral images. Variations of these models have used pinhole lenslets³ eliminating aberrations, along with simplified algorithms of minimal computational requirements that provide IP images rendered in real time. However, the main drawback of such an approach is a significant quality degradation of the generated IP images, thus constraining its practical use in rudimentary 3-D applications. Most recently, full aperture lens modeling has been proposed,⁴ taking into account lens aberrations and using basic ray tracing algorithms to overcome these limitations. In addition, interpolative shading techniques have been used⁴ for improved realism of the generated IP images. These techniques provide integral images of adequate quality but have restrictions in the complexity of the 3-D scenes, while the employed ray tracing algorithms are simplified and mostly focused to the generation of IP images with horizontal parallax (lenticular integral photography).

A similar methodology, referred in the literature as “autostereoscopic light fields,” uses a lens array for direct viewing of light fields.⁵ In the corresponding article, a detailed analysis is given concerning focusing and depth of field problems. However, the reconstruction stage is shortly covered with no reference to pseudoscopy elimination and the required gap between the lens array and the display panel to clearly differentiate between real and virtual 3-D scenes.

Paper 05128R received Jul. 7, 2005; revised manuscript received Apr. 13, 2006; accepted for publication May 4, 2006. This paper is a revision of a paper presented at the SPIE conference on Stereoscopic Displays and Virtual Reality Systems XII, Jan. 2005, San Jose, California. The paper presented there appears (unrefereed) in SPIE Proceedings Vol. 5664. 1017-9909/2006/15(4)/1/0/\$22.00 © 2006 SPIE and IS&T.

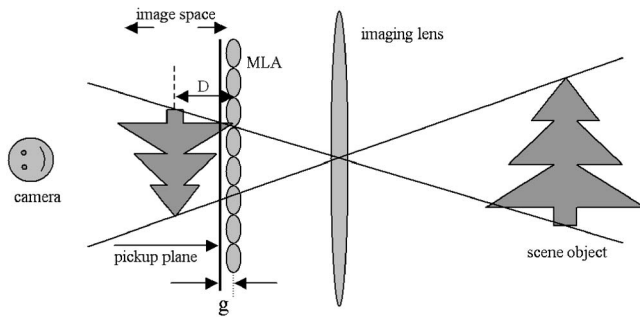


Fig. 1 Single-stage IP capturing setup for production of real and virtual images (distances not in scale).

The objective of this work is to propose a computer simulation of a physically implemented single-step integral imaging capture scheme,⁶ using the POV-Ray software package as the ray tracing engine.⁷ The simulation of the capturing optics has been realized by modeling the microlens array as an ordinary object of the 3-D scene⁸ using the ray tracer's scene description scripting language. This approach takes advantage of the optimized algorithms implemented in POV-Ray to produce high quality photorealistic 3-D images. Moreover, it provides great flexibility for the optimal specification of critical design parameters of the capturing and reproduction optics as the pitch size of the microlenses and the number of pixels under each microlens, thus supporting various display resolutions in an elegant way.

Furthermore, an additional imaging lens is modeled⁸ as part of our capturing setup. With this imaging lens, we have the ability to capture virtual and real pseudoscopic IP images by proper placement of the lens array in the image space of the 3-D scene. The captured images are then processed with a pseudoscopy elimination algorithm, resulting in real and virtual orthoscopic IP images. At the reconstruction stage, a lens array is placed on top of the IP image, and the reconstructed 3-D scene is formed in space in front of the lens array or behind it.

In the following sections, first we provide an analysis of the modeled single-stage IP capturing setup, followed by the physical modeling methodology applied for all the optical components. Experimental results along with an extension of the proposed method to integral videography are then presented, followed by conclusions and future work.

2 Single-Stage Integral Photography Capturing Setup for Real and Virtual Images

The single-stage IP capturing setup⁶ that has been physically implemented with POV-Ray^{7,8} is depicted in Fig. 1. In this setup, the imaging lens forms an inverted and demagnified real image of the original 3-D scene. An important advantage of this capturing system is that both real and virtual integral images can be produced depending on the position of the microlens array (MLA) in the resulted image space.

The produced integral images are pseudoscopic because of the inversed depth phenomenon that is inherent in a single-stage IP capturing system. These pseudoscopic images are then computationally converted to orthoscopic

ones by performing an 180-deg rotation of each elemental image (that is, the subimage that corresponds to each microlens) around its optical axis.⁹

The relative distance D of the MLA in regard to the central plane of the image space determines which parts of the IP image are real or virtual. When the MLA is positioned at the end of the image space toward the imaging lens, as in Fig. 1, a virtual pseudoscopic integral image is produced and the pickup integral image is formed at the pickup plane at a distance g from the MLA, which is approximately equal to its back focal length. After the pseudoscopy elimination procedure, a real orthoscopic integral image is produced. At the reconstruction stage, the 3-D scene floats in space in front of the MLA toward the observer. This kind of 3-D reconstruction is more attractive and realistic to the observer than a virtual one,⁶ and for this reason it has been selected for realization in the modeled capturing setup.

Alternatively, when the MLA is placed at the end of the image space toward the camera, the captured integral image is real pseudoscopic, and the final outcome after pseudoscopy elimination is a virtual orthoscopic integral image. At the reconstruction stage, such an image is formed behind the MLA. By placing the MLA within the image space, the modeled IP capturing system is able to produce both real and virtual integral images.

3 Physical Modeling Methodology

All optical components of the capturing IP setup are modeled using the ray tracer's scene description language. The geometrical and optical characteristics of the plano-convex lenses are taken into account and constructive solid geometry (CSG) techniques are used for the construction of each microlens and the microlens arrays.

3.1 Microlens Array Model

Microlens structures typically used in integral photography are square or hexagonal-shaped planoconvex microlenses with spherical curvature and constant index of refraction exhibiting higher fill factors than other structures, such as spherical microlenses. Gradient index microlens arrays have also been proposed,¹⁰ but their fabrication is more difficult, making them a very expensive solution for the reconstruction stage compared with the previously referenced structures. Therefore, for MLA modeling we have adopted plano-convex microlenses with spherical curvature and square or hexagonal shape. The optical parameters that are needed for the construction of each microlens of the MLA are the index of refraction n of the microlens material and its focal length f . The radius of curvature R can be calculated from n and f using the lensmaker's formula, which in the case of a plano-convex lens is given by:

$$R = (n - 1)f. \quad (1)$$

Each microlens is formed as the intersection of a sphere and a parallelepiped or a hexagonal prism to produce square or hexagonal lenslets, respectively. In either case, the formed microlenses are fully apertured and the radius R of the sphere corresponds to the radius of curvature of the convex surface. Modeling of thin lenslets has been accomplished by properly adjusting the relative positions of the

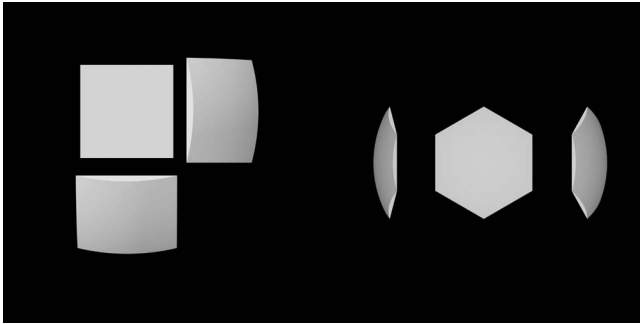


Fig. 2 3-D views of simulated microlenses (a) square-based and (b) hexagonal-based.

parallelepiped or the hexagonal prism and the sphere. For square microlenses, the displacement d of the parallelepiped from the center of the sphere is calculated using the following equation, which is derived from the geometry of the intersection of the sphere and the parallelepiped, where p is the pitch of the microlens array:

$$d = [(R)^2 - (p/2)^2]^{1/2}. \quad (2)$$

For hexagonal microlenses, the displacement d of the hexagonal prism from the center of the sphere is calculated using the following equation, which is derived from the geometry of the intersection of the sphere and the hexagonal prism:

$$d = \left[(R)^2 - \left(\frac{p}{2 \cos(30 \text{ deg})} \right)^2 \right]^{1/2}. \quad (3)$$

The 3-D structures of the modeled square and hexagonal microlenses are shown in Figs. 2(a) and 2(b), respectively.

Each lens array has been formed as a CSG union of a symmetrical grid of microlenses. The two types of microlens arrays that have been formed in this way are depicted in Figs. 3 and 4, respectively.

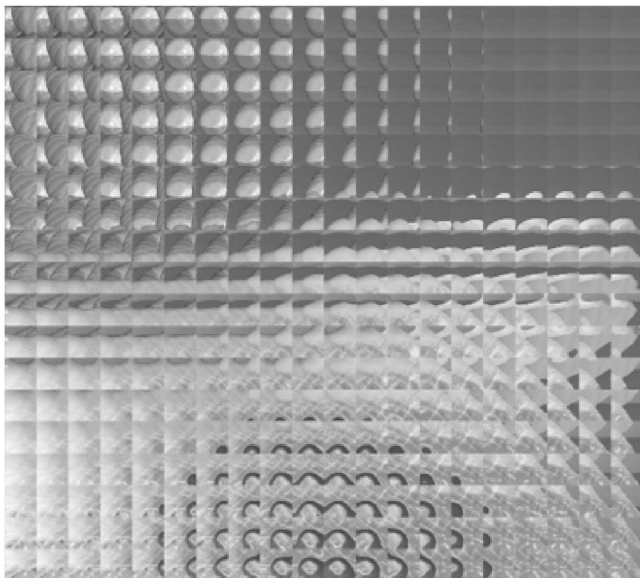


Fig. 3 Sample capture using square lens array

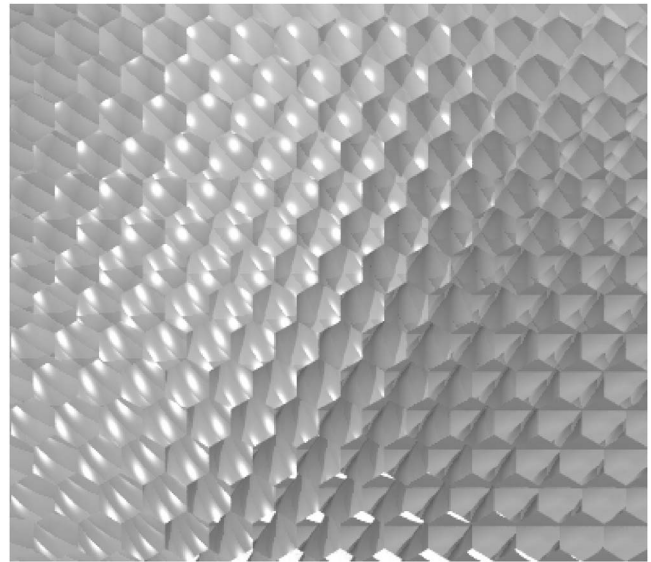


Fig. 4 Sample capture using hexagonal lens array.

For the reconstruction stage, IP is very demanding in resolution requirements to produce high quality 3-D images.⁹ Therefore, LCDs with resolutions on the order of 200 dpi or high resolution printers must be used in combination with the appropriate MLA. To demonstrate the high quality and photorealism of the integral images produced, we have utilized a color ink-jet printer (2400 × 1200 dpi). The dimensions of the IP image have been chosen to be about 10 × 10 cm, so that a fairly complicated 3-D scene can be presented with enough depth for an adequate 3-D sensation. Considering a printer resolution of 600 dpi and microlenses of 1-mm pitch, we have used a ray tracer output window of 2400 × 2400 pixels corresponding to an MLA of 100 × 100 microlenses for the capturing of the 3-D scene.

3.2 Imaging Lens Setup

The imaging lens that is typically used for IP capturing^{6,10} is a large aperture biconvex lens. One such imaging lens was modeled in the ray tracer, resulting in increased geometrical aberrations. To reduce these aberrations, we have examined the predominant factors that produced them. The most important was the effect of the nonparaxial rays, and for this reason we have substantially restricted ray tracing to paraxial rays by empirically using a viewing angle of about 1/10 of the default-viewing angle for the perspective camera model.

As for the imaging lens structure, a well-corrected physically based camera model has been proposed for computer graphics,¹¹ which offers a superior optical performance but uses a large number of optical elements. However, the modeling of a complex imaging lens substantially increases rendering time, since the required size of the 3-D image captured must be comparable to the MLA size for optimal results. Therefore, we have used a simpler imaging lens model, specifically a condenser optical system consisting of two identical large aperture plano-convex lenses with their convex vertices in contact. This system has been extended with the use of an additional thick plano-convex

Table 1 Design details of the modeled imaging lens. Each row in the table describes a surface of a lens element, listed in order from object space to image space. The first column is the surface number, followed by the signed radius of curvature of the spherical element, the thickness (distance between two successive surfaces), the index of refraction of the material, and the semiaperture of the surface element (all units are in centimeters).

Surface	Radius	Thickness	Glass (index of refraction)	Semiaperture
1	Infinity	08.428	1.51	10
2	-24.238	28.930		10
3	Infinity	01.716	1.50	10
4	-30.000	0		10
5	+30.000	01.716	1.50	10
6	Infinity			10

lens, and the resulted optical system has been used as part of the capturing setup. The optical parameters of the modeled imaging system have been specified using the ZEMAX optical design software package and the design details are given in Table 1. It should be noted that the implementation of a simple lens structure with only three elements resulted in barrel distortions, which were minimized using a median lateral magnification of 1/5 for the imaging lens.

The modeling was based on geometrical optics and did not cover wave-optics effects. Furthermore, chromatic aberrations were not taken into account. Regarding image formation, the algorithms used for the computation of the ray-transfer matrix of the imaging lens were implemented in POV-Ray as the product of the ray-transfer matrices of all the surfaces included.¹² The optical system parameters were then determined from the ray-transfer matrix. The system focal length f was calculated to be 30 cm. This resulted in an imaging lens with an f-number of 1.5 at full aperture. To get a real inverted and demagnified 3-D scene image, we have retained a minimum distance of 100 cm between the front end of the 3-D scene and the imaging system, which was much greater than $2f$. Furthermore, for realistic results, the depth of the 3-D scene has been set to 150 cm, large enough to capture IP images that exhibit both real and virtual parts with respect to the median image plane.

For system completeness, a variable aperture has been realized by appropriate modeling and has been included in the imaging lens. Regarding matching of the imaging lens and microlens f-numbers,¹⁵ the microlens f-number was 3.3, while the imaging lens f-number was 1.5 at full aperture. In a real IP capturing setup, an image sensor must be placed behind the lens array at a distance equal to the back focal length of the microlenses. In that case, a certain number of sensor pixels fall behind each microlens. Mismatched f-numbers, specifically when the f-number of the imaging lens is less than the f-number of the microlenses, cause pixel overflow of each microimage to adjacent ones and the appearance of cross talk. However, our setup was a synthetic capturing and not a real IP capturing setup. Capturing was accomplished utilizing the camera model of

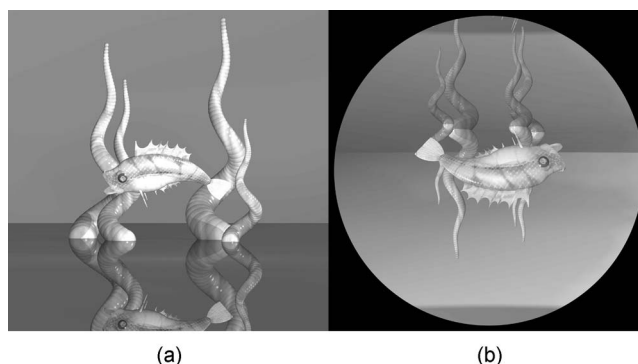


Fig. 5 (a) test 3-D scene and (b) 3-D scene image after the imaging lens.

POV-Ray, which is a pinhole camera with an infinite depth of field. This camera model captures the IP image formed behind the lens array at the proximity of its back focal length, keeping everything in focus, resulting in IP images that do not exhibit cross talk. Moreover, by stopping down, the imaging lens would result in fewer pixels under each microlens that records the 3-D information. Therefore, in our setup the imaging lens has been set to full aperture.

4 Experimental Results

The modeled IP capturing system has been tested using a 3-D scene of increased complexity, and real and virtual orthoscopic images have been produced. In addition, an extension of this method has been performed for the generation of 3-D videos (integral videography).

4.1 Three-Dimensional Scene Capturing and Reconstruction Setup

A sample scene for evaluation has been selected from the advanced scene examples of POV-Ray with minor modifications, as depicted in Fig. 5(a).

In this scene a fish exists in the air above a water surface. The fish skin and its eyes are textured with image maps. Two stems have been positioned behind the fish and at a distance, having different depths but close to each other. Two omnidirectional light sources have been used in the scene. The fish and stems are reflected in the water underneath them. A slight modification has been applied to this scene by adding three more omnidirectional light sources along with two more stems behind the fish. These additions have been made to increase the complexity of the scene, thus creating a 3-D scene containing a total of five lights and four stems, as depicted in Fig. 5(a) (front view) and Fig. 6 (side view). Furthermore, the 3-D scene depth, that is, the distance between the fish and the last stem, has been significantly increased to exhibit the capturing of mixed real and virtual IP images.

The detailed setup that has been modeled is depicted in Fig. 6. The imaging lens was a composition of three plano-convex large aperture lenses, as already described. The distance of the 3-D scene to the imaging lens was 100 cm, while the depth of the 3-D scene was 150 cm. The image of the 3-D scene has been formed at 13.42 cm from the imaging lens with a depth of 5 cm (a depth compression factor

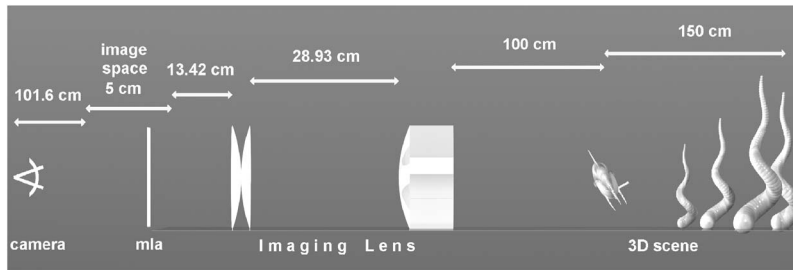


Fig. 6 Single stage IP capturing setup for production of real and virtual orthoscopic images (distances and object lengths not in scale).

of 30). However, since the lateral and depth magnifications of the imaging lens were significantly different, the final reconstructed 3-D scene was distorted.

By using a specific lens array in the reconstruction stage, the resolution of the display device determines the number of pixels under each microlens. In the capturing stage, the same number of pixels can be realized by properly choosing the distance between the camera and the microlens array while keeping a constant viewing angle. Therefore, the accurate estimation of the camera position results in an exact pixel arrangement under each successive microlens.

Moreover, the position of the MLA within the image space controls the type of IP images that will be produced (real or virtual). Synthetic captured IP images for four successive MLA positions relative to the central plane of the fish body are shown in Figs. 7(a) through 7(d) to demonstrate the transition from real to virtual 3-D images. The integral images have been rendered using a window size of 2400×2400 pixels with 23 and 24 pixels under each microlens in an alternating sequence.

The reconstruction of the 3-D scene has been realized by printing or displaying the captured integral images in combination with the appropriate MLA. The specifications of the MLA used in the reconstruction stage should better match those of the modeled MLA in the ray tracer.¹⁴ The use of the same MLA in the reconstruction as the one modeled results in a 3-D scene identical to the one sampled by the MLA. A virtual 3-D image was formed at a certain depth behind the display panel and exhibited smooth parallax, while a real 3-D image floated in space in front of the display panel. In the latter case, the 3-D scene appeared more attractive and realistic. The resolution of the reconstructed 3-D image depends strongly on its depth, and image quality deteriorates as image depth increases. Therefore, to produce a high quality photorealistic 3-D image, it is often preferable to combine a real and virtual 3-D image with a reasonable depth.

The relative distance between the MLA and the central plane of the image space controls the type of IP images that will be produced (real or virtual). By positioning the MLA at the end of the image space toward the imaging lens, a virtual pseudoscopic image is produced, which is finally translated to a real orthoscopic one.^{6,8} Considering an MLA with a focal length f , at the reconstruction stage the gap g_r between the lens array and the display plane must be greater than f , resulting in an image that is formed in front of the display plane. Alternatively, by positioning the MLA at the other end of the image space (toward the camera), a

real pseudoscopic image is produced, which is finally translated to a virtual orthoscopic image. Accordingly, for this case the gap g_v between the lens array and the display plane must be less than f , resulting in an image that is formed behind the display plane.

In the work presented, the MLA modeled in the capturing setup has followed the specifications of item 630 of Fresnel Technologies,¹⁵ which is a rectangular lens array

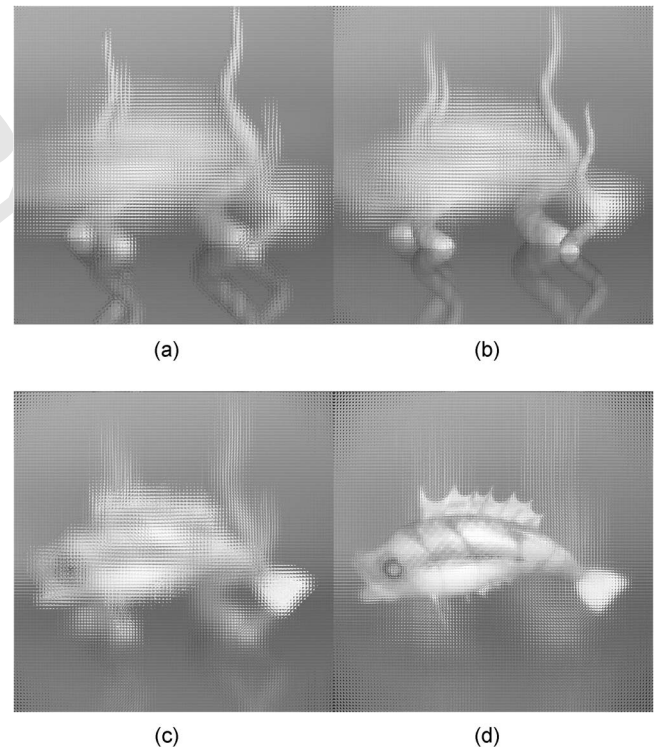


Fig. 7 IP images captured by varying the MLA position at different depths within the 3-D image space. All distances refer to the central plane of the fish image. (a) MLA at 6 cm toward the imaging lens (the MLA is in front of the image space, therefore, at the reconstruction stage, the whole 3-D image is formed in front of the MLA—orthoscopic real image), (b) MLA at 4 cm toward the imaging lens (the fish is formed in front of the MLA, while the stems are formed just behind the MLA), (c) MLA at 1 cm toward the imaging lens (the fish is formed just in front of the MLA, while the stems are formed behind the MLA), and (d) MLA at 1 cm toward the camera (the MLA is behind the image space, therefore, at the reconstruction stage, the whole 3-D image is formed behind the MLA—orthoscopic virtual image).

with 3.3-mm focal length and 1-mm pitch. This lens array has a substrate thickness equal to its focal length. Targeting to a high-resolution printer of 600 dpi for the reconstruction, we have captured IP images with 23 or 24 pixels in an alternating sequence under each microlens. The images thus generated have been processed for pseudoscopy elimination, and then printed on premium photo-quality paper using a high-resolution inkjet printer (HP DeskJet 1220C). At the reconstruction stage, the lens array has been placed over the printed IP images at predetermined gaps. Real orthoscopic images have been observed using a gap g_r of 4.8 mm (including the substrate thickness of 3.3 mm), while for the reconstruction of virtual orthoscopic images, the gap g_v was equal to the focal length of the decoding MLA due to its substrate thickness.

For the reconstruction stage, it is evident that a real orthoscopic 3-D scene that is formed in space and in front of the lens array cannot be easily presented using conventional 2-D photography techniques. However, the 3-D information contained in each IP image, as those depicted in Fig. 7, can be shown indirectly using an IP viewer that downsamples the captured IP images by appropriate spatial filtering of the corresponding pixel information under each microlens or adjacent microlenses, resulting in 2-D views for different viewing angles or depths. Sequences of different views of the 3-D scene extracted from a single IP image were generated with this viewer and are presented in Ref. 16.

4.2 Integral Videography

Integral videography (IV) is an animated extension of integral photography. The motivation for IV, except for the obvious 3-D applications, has resulted from the need to have a controllable source of 3-D videos for studying novel video compression techniques, which is of vital importance due to the high resolution of the IV frames needed and the associated huge volumes of data. In what follows, the parameters affecting frame rendering time and a 2-D representation of the information contained in the computer-generated IV frames are addressed.

4.2.1 Parameters affecting frame-rendering time

As in normal video, an IV movie is produced as a sequence of integral images in time. However, in IV, the primary parameter affecting the quality of the reconstructed 3-D scene is the resolution of the display device used. For IP reconstruction, the MLA pitch determines the lateral resolution of the 3-D scene produced. A microlens pitch close to 1 mm seems to be a good compromise between the acceptable spatial discrimination for an observer at a maximum viewing distance of 1 m and the required resolution for the display device. As a rule of thumb, the number of pixels under each microlens for acceptable IP images must be on the order of 10×10 . However, with maximum resolutions of 200 dpi that are currently available for LCD screens, an acceptable quality can be achieved using 8×8 pixels under each microlens with a 1-mm pitch MLA.

In the reconstruction setup, we have used a high-resolution LCD screen of 203 dpi along with a 1-mm pitch rectangular lens array. This arrangement resulted in 8×8 pixels under each microlens. By keeping the total number of microlenses at the same levels as in the IP capturing

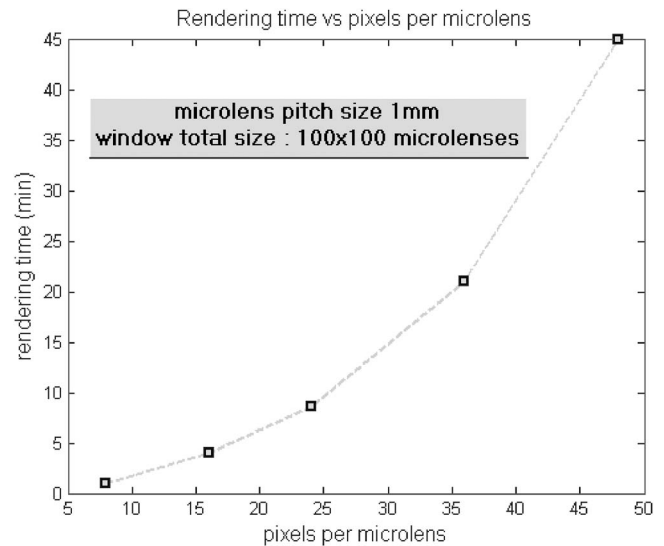


Fig. 8 Rendering time results versus number of pixels per microlens. A total of 100×100 microlenses are used for each render. The MLA has 1-mm pitch size. Antialiasing is off.

setup, the reduction of 1/3 in the number of pixels under each microlens resulted in an analogous reduction in the total window size. Therefore, there was a significant decrease in rendering time, as depicted in Fig. 8.

In the IVs presented,¹⁶ we have modeled a 90×90 microlens array with a resolution of 8×8 pixels per microlens, resulting in a rendered window of 720×720 pixels.

Another important issue regarding IV was the use of the ray tracer antialiasing options. Rendering time was greatly affected from antialiasing because of the increased number of supersamples used. In Fig. 9, we depict the variation of rendering time versus antialiasing threshold in POV-Ray, which is a parameter inversely proportional to the number of supersamples.⁷ The capturing setup for IV has been modeled on a PC system with a Pentium 4 CPU at 3 GHz with 1-Gbyte memory. As supersampling was increased (antialiasing threshold decreased), rendering time increased rapidly, as depicted in Fig. 9, resulting in smooth microimages with no clear borders, while with no antialiasing, the microimage borders could be clearly identified. However, for pseudoscopy elimination, it was important to determine with precision the borders of each microimage. Therefore, as a tradeoff exists between microimage smoothness, pseudoscopy elimination, and rendering time, we did not utilize the antialiasing options for the IVs generated.

4.2.2 Three-dimensional information contained within each frame

Each IV frame is substantially different in nature from a typical video frame, since 3-D information is embedded. Therefore, in an IV video in which the camera is still and the object is moving, the number of pixels under each microlens and the MLA size define the amount of 3-D information enclosed in each IV frame. In Figs. 10(a) and 10(b), two successive IV frames are depicted in which the 3-D scene consists of the fish body that is turning horizontally around its axis by 8 deg per frame. In what follows, and to present in a conventional display the 3-D videos generated,

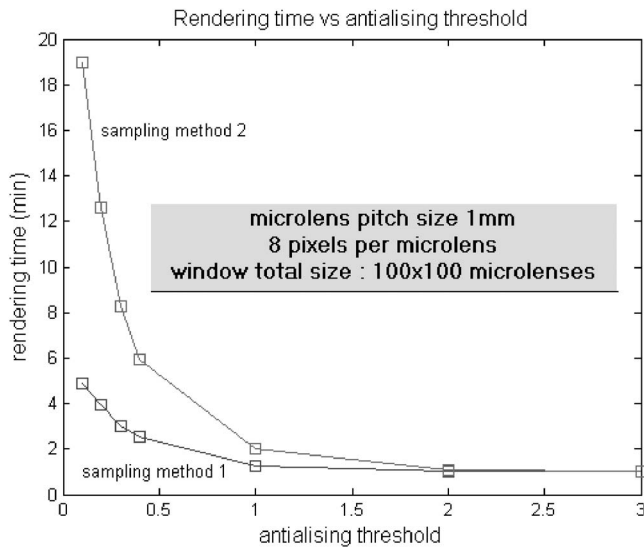


Fig. 9 Rendering time results versus antialiasing threshold. A total of 100×100 microlenses are used for each render. A rect. MLA is used with 1-mm pitch size. Antialiasing threshold 3 corresponds to antialiasing off. Sampling method 1 is an adaptive, nonrecursive, supersampling method. Sampling method 2 is an adaptive, recursive, supersampling method with control over the maximum number of samples taken for a supersampled pixel (we have set the corresponding depth-control parameter to 3).

we have extracted 2-D views of the 3-D scene for each IV frame. This has been accomplished by downsampling the corresponding IV frame by appropriate spatial filtering of the pixel information under each microimage. The resulting view size depends on the total number of microlenses capturing the IP image. The number of different views that can be extracted in each direction (horizontal or vertical) depends on the number of pixels under each microlens.

Using the two successive IV frames of Fig. 10, we can directly extract 16 2-D views, from which six equally spaced in time views are shown in Figs. 11(a) through 11(f). The two successive IV frames depicted in Figs. 10(a) and 10(b) as well as a sequence of all successive views extracted from these two IV frames, combined into one movie, are available in Ref. 16.

5 Conclusions and Future Work

A novel way for producing high quality, photorealistic integral images of complex 3-D scenes is proposed, using an advanced general-purpose ray tracing software package. With this approach, all necessary optics are modeled like

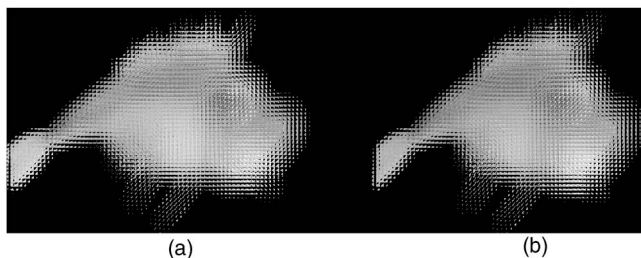


Fig. 10 Successive IV frames. The fish is turning horizontally clockwise around its axis. Camera is still.

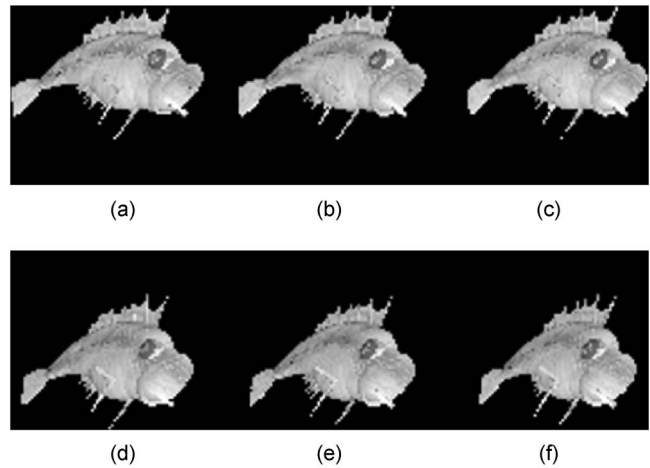


Fig. 11 Successive views extracted from an IV sequence. Views (a), (b), and (c) are the extreme left, middle, and extreme right views extracted from the IV frame in Fig. 10(a). Views (d), (e), and (f) are the extreme left, middle, and extreme right views extracted from the IV frame in Fig. 10(b).

ordinary objects of the 3-D scene. This methodology constitutes a source of IP images and IVs with controllable 3-D content for developing new compression techniques for 3-D still images¹⁷ and videos, and studying the reconstruction stage concerning viewing angle and depth.

The proposed methodology offers full depth control and positioning of the reconstructed 3-D scene. Besides, the modeling of an MLA using real world parameters further ensures that the reconstructed 3-D scene has optimum quality. In addition, the proposed technique has the advantage of allowing the combination of real and virtual IP images for autostereoscopic viewing of complex photorealistic 3-D scenes exhibiting mixed depth in front and behind the display device. The methodology presented can be easily extended to integral videography, producing high quality 3-D videos along with depth control.

Currently, raster graphics are the dominating technology used for computer graphics, but the rendered images can hardly reach the photorealism achieved with ray tracing techniques, especially for more advanced 3-D scenes.¹⁸ Ray tracing has increased computational cost compared to raster graphics. However, as the complexity of the 3-D scene increases, the ray tracing approach takes advantage over raster graphics concerning computational requirements,¹⁹ thus it is expected that hardware accelerated ray traces will prevail in the future in computer graphics.^{18,20} In this context, the proposed methodology is expected to be of significant importance for computer generated 3-D display techniques. However, more work should be done in modeling physically realizable, well-corrected lens systems of increased complexity,¹¹ especially in the case of modeling MLAs with sizes comparable to CCDs. In addition, an important drawback of the proposed ray tracing approach is that the rendering time is far from considered real time, thus hardware-accelerated ray tracing techniques should be considered.^{18,20}

Acknowledgments

This research was co-funded by 75% from E.C. and 25% from the Greek Government under the framework of the Education and Initial Vocational Training Program—Archimedes. Furthermore, we would like to express our thanks to I. Antoniou, S. Dudnikov, Y. Melnikov, and A. Dimakis for their contribution to our work, through the TDIS Project, which was funded from E.C..²¹

References

1. G. Lippmann, "La photographie integrale," *Comptes-Rendus Academie des Sciences*, **146**, 446–451 (1908).
2. B. Lee, S. W. Min, S. Jung, and J. H. Park, "A three-dimensional display system based on computer-generated integral photography," *J. Soc. 3D Broadcast. Imag.*, **1**(1), 78–82 (2000).
3. Y. Igarashi, H. Murata, and M. Ueda, "3D display system using a computer generated integral photograph," *Jpn. J. Appl. Phys.*, **17**, 1683–1684 (1978).
4. G. Milnthorpe, M. McCormick, and N. Davies, "Computer modeling of lens arrays for integral image rendering," *IEEE Computer Society, Proc. EGUK'02*, 136–141 (2002).
5. A. Isaksen, L. McMillan, and S. J. Gortler, "Dynamically reparameterized light fields," *SIGGRAPH '00 Proc.*, pp. 297–306 (2000).
6. J. S. Jang and B. Javidi, "Formation of orthoscopic three-dimensional real images in direct pickup one-step integral imaging," *Opt. Eng.*, **42**(7), 1869–1870 (2003).
7. See <http://www.povray.org>.
8. S. Athineos, N. Sgouros, P. Papageorgas, D. Maroulis, M. Sangriotis, and N. Theofanous, "Physical modeling of a microlens array setup for use in computer generated IP," *Proc. SPIE* **5664**, 472–479 (2005).
9. T. Okoshi, *Three Dimensional Imaging Techniques*, Academic Press, New York (1971).
10. J. Arai, F. Ocano, H. Hoshino, and I. Yuyama, "Gradient-index lens array method based on real-time integral photography for three-dimensional images," *Appl. Opt.*, **37**(11), 2034–2045 (1998).
11. C. Kolb, D. Mitchell, and P. Hanrahan, "A realistic camera model for computer graphics," *Computer Graphics SIGGRAPH '95 Proc.*, pp. 317–324 (1995).
12. J. W. Goodman, *Introduction to Fourier Optics*, 3rd ed., Appendix B, Roberts and Company (2005).
13. Stanford technical report; <http://graphics.stanford.edu/papers/lfcamera>.
14. J. H. Park, H. Choi, Y. Kim, J. Kim, and B. Lee, "Scaling of three-dimensional integral imaging," *Jpn. J. Appl. Phys., Part 1* **44** (1A), 216–224 (2005).
15. Fresnel Technologies, See <http://www.fresneltech.com>
16. See: <http://imaging.di.uoa.gr>.
17. N. Sgouros, A. Andreou, M. Sangriotis, P. Papageorgas, D. Maroulis, and N. Theofanous, "Compression of IP images for autostereoscopic 3D imaging applications," *IEEE 3rd Intl. Symp. Image Signal Process. Anal. (ISPA)*, pp 223–227 (2003).
18. S. Woop, J. Schmittler, and P. Slusallek, "RPU: a programmable ray processing unit for realtime ray tracing," *ACM Trans. Graphics*, **24**(3), 434–444 (2005).
19. J. Hurley, "Ray tracing goes mainstream," *Intel Technol. J.*, **09**(02), 99–107 (2005), See <http://developer.intel.com/technology/itj/index.htm>.
20. J. Fender and J. Rose, "A high-speed ray tracing engine built on a field-programmable system," *IEEE Intl. Conf. Field-Programmable Technol.*, pp. 188–195 (2003).
21. TDIS, See http://icadc.cordis.lu/fep-cgi/srchidadb?ACTION=D&CALLER=PROJ_IST&QM_EP_RCN_A=64022.

Biographies and photographs of authors not available.